

# Structural Bone Deficits in HIV/HCV-Coinfected, HCV-Monoinfected, and HIV-Monoinfected Women

Vincent Lo Re III,<sup>1,3,4</sup> Kenneth Lynn,<sup>1,3</sup> Emily R. Stumm,<sup>1,3</sup> Jin Long,<sup>6</sup> Melissa S. Nezamzadeh,<sup>4</sup> Joshua F. Baker,<sup>2</sup> Andrew N. Hoofnagle,<sup>8</sup> Angela J. Kapalko,<sup>7</sup> Karam Mounzer,<sup>7</sup> Babette S. Zemel,<sup>5</sup> Pablo Tebas,<sup>1,3</sup> Jay R. Kostman,<sup>1,3</sup> and Mary B. Leonard<sup>4,9</sup>

Divisions of <sup>1</sup>Infectious Diseases, <sup>2</sup>Rheumatology, Department of Medicine, <sup>3</sup>Center for AIDS Research, <sup>4</sup>Center for Clinical Epidemiology and Biostatistics, Department of Biostatistics and Epidemiology, <sup>5</sup>Division of Gastroenterology, Hepatology, and Nutrition, Department of Pediatrics, Perelman School of Medicine, University of Pennsylvania, and Children's Hospital of Philadelphia, <sup>6</sup>Healthcare Analytics Unit, Children's Hospital of Philadelphia, and <sup>7</sup>Jonathan Lax Treatment Center, Philadelphia FIGHT, Pennsylvania; <sup>8</sup>Department of Laboratory Medicine, University of Washington, Seattle; and <sup>9</sup>Department of Pediatrics and Medicine, Stanford University, California

**Background.** Coinfection with human immunodeficiency virus (HIV) and hepatitis C virus (HCV) is associated with reduced bone mineral density (BMD) and increased fracture rates, particularly in women. The structural underpinnings for skeletal fragility in coinfecting women have not been characterized. We used tibial peripheral quantitative computed tomography to evaluate skeletal parameters in women, by HIV/HCV status.

**Methods.** We conducted a cross-sectional study among 50 HIV/HCV-coinfecting, 51 HCV-monoinfecting, and 50 HIV-monoinfecting women. Tibial volumetric BMD and cortical dimensions were determined with peripheral quantitative computed tomography. Race-specific *z* scores for age were generated using 263 female reference participants without HIV infection or liver disease.

**Results.** Coinfecting participants had lower mean *z* scores for trabecular volumetric BMD (−0.85), cortical volumetric BMD (−0.67), cortical area (−0.61), and cortical thickness (−0.77) than reference participants (all *P* < .001). The smaller cortical dimensions were due to greater mean *z* scores for endosteal circumference (+0.67; *P* < .001) and comparable *z* scores for periosteal circumference (+0.04; *P* = .87). Trabecular volumetric BMD was lower in coinfecting than in HCV- or HIV-monoinfecting participants. HCV-infected women with stage 3–4 liver fibrosis had lower mean *z* scores for trabecular volumetric BMD, cortical thickness, and total hip BMD those with stage 0–2 fibrosis.

**Conclusions.** Compared with healthy reference patients, HIV/HCV-coinfecting women had decreased tibial trabecular volumetric BMD, diminished cortical dimensions, and significant endocortical bone loss.

**Keywords.** bone; hepatitis C virus; HIV; coinfection; peripheral quantitative computed tomography.

Low bone mineral density (BMD) is a recognized metabolic complication of human immunodeficiency virus (HIV) [1, 2] and chronic hepatitis C virus (HCV) infection [3, 4]. Among HIV-infected patients, BMD further

decreases 2%–6% during the first 2 years of antiretroviral therapy (ART) [5–7]. Each of these chronic infections has been associated with an increased risk of fracture compared with uninfected persons [8–10]. HCV coinfection is associated with further reductions in BMD in HIV-infected patients [11–14], particularly women [11, 12, 14]. Rates of hip fracture are also significantly higher in HIV/HCV-coinfecting than in HIV-monoinfecting, HCV-monoinfecting, and uninfected persons [10].

Various factors related to HIV and chronic HCV have been hypothesized to contribute to skeletal fragility. HIV-related inflammation, ART-related toxicity, increased prevalence of tobacco or alcohol use, and established osteoporosis risk factors exacerbated by HIV contribute to

Received 4 December 2014; accepted 2 March 2015; electronically published 9 March 2015.

Presented in part: ID Week 2014, Philadelphia, Pennsylvania, 8–12 October 2014. Oral abstract 645.

Correspondence: Vincent Lo Re III, MD, MSCE, Center for Clinical Epidemiology and Biostatistics, University of Pennsylvania School of Medicine, 836 Blockley Hall, 423 Guardian Dr, Philadelphia, PA 19104-6021 (vincentl@mail.med.upenn.edu).

The Journal of Infectious Diseases® 2015;212:924–33

© The Author 2015. Published by Oxford University Press on behalf of the Infectious Diseases Society of America. All rights reserved. For Permissions, please e-mail: journals.permissions@oup.com.

DOI: 10.1093/infdis/jiv147

low BMD and increased fracture risk in persons with HIV infection [15]. Inflammatory cytokines associated with chronic HCV, particularly tumor necrosis factor (TNF)  $\alpha$ , interleukin-1 (IL-1), and interleukin-6 (IL-6), might inhibit bone formation and increase bone resorption [16, 17]. The development of HCV-related hepatic decompensation might further contribute to a decrease in BMD by impairing the production of factors (eg, 25-hydroxyvitamin D [25(OH)D], insulinlike growth factor 1) that promote bone formation and mineralization [3, 4].

Despite the observed decrements in BMD [11–14] and increased fracture risk among HIV/HCV-coinfected individuals [10], the structural underpinnings and mechanisms for the skeletal fragility in these patients have not been established. Studies of BMD in coinfecting patients have relied exclusively on dual-energy x-ray absorptiometry (DXA), a 2-dimensional projection technique that summarizes total trabecular and cortical bone mass within the projected bone area. DXA is therefore unable to identify distinct deficits within trabecular and cortical bone. Peripheral quantitative computed tomography (pQCT) provides 3-dimensional estimates of trabecular and cortical volumetric BMD and cortical geometry in the appendicular skeleton that are highly correlated with failure load [18, 19]. Characterization of trabecular and cortical bone deficits and associated metabolic and body composition abnormalities in HIV/HCV-coinfected patients can suggest potential mechanisms of bone loss and inform future studies of bone therapies in this at-risk and aging population. We performed tibial pQCT and whole-body DXA in ART-treated HIV/HCV-coinfected women compared with HCV-monoinfected women, ART-treated HIV-monoinfected women, and healthy women without a history of HIV infection or viral hepatitis. Our analyses focused on women because associations between HIV/HCV coinfection and low BMD have been stronger in women than in men [12, 14]. We hypothesized that coinfecting women would have lower trabecular volumetric BMD and cortical thinning due to endocortical bone loss, a pattern observed in other chronic inflammatory diseases [20–22], compared with HCV- or HIV-monoinfected women and those without a history of either infection.

## METHODS

### Study Design and Setting

We performed a cross-sectional study among ART-treated HIV/HCV-coinfected, HCV-monoinfected, and ART-treated HIV-monoinfected women recruited from infectious diseases and hepatology practices at the Hospital of the University of Pennsylvania, Penn Presbyterian Medical Center, and Jonathan Lax Center, 3 centers affiliated with the University of Pennsylvania in Philadelphia. These practices provide HIV and HCV care to all 3 patient groups. The study was approved by the institutional review boards of the University of Pennsylvania and Jonathan Lax Center. Informed consent was obtained from all participants.

### Study Participants

All study participants were aged  $\geq 18$  years. Other eligibility criteria were as follows: HIV-monoinfected women, (1) stable ART regimen for 3 months, (2) HIV RNA  $< 1000$  copies/mL (suggesting controlled HIV infection), and (3) negative results for HCV antibody; HCV-monoinfected women, (1) detectable HCV RNA, (2) HCV genotype 1 (predominant genotype in the United States and western Europe [23, 24]), (3) hepatic fibrosis staging by liver biopsy or noninvasive test within 2 years before enrollment, and (4) negative results for HIV antibody; HIV/HCV-coinfected women, criteria 1–2 for HIV-monoinfected and 1–3 for HCV-monoinfected participants. Liver fibrosis assessment was required for HCV-infected participants because we wanted to assess bone and body composition measurements by hepatic fibrosis stage.

Exclusion criteria were as follows: (1) active opportunistic infection, malignancy, hepatic decompensation, or substance abuse within 3 months of enrollment (conditions that can alter body composition and/or bone mass [3, 4, 25]); (2) previous HCV therapy (which can affect BMD [26]); or (3) pregnancy or breastfeeding (to avoid radiation exposure). We targeted a sample size of 50 participants per group to provide 80% power to detect a difference in  $z$  score of 0.5 between the groups, which we considered clinically significant.

Reference data were generated in 263 women (aged 21–78 years) in a prior study of bone and body composition using the same pQCT and DXA machines and methods [27]. These participants were recruited from Hospital of the University of Pennsylvania and Penn Presbyterian Medical Center clinics and the surrounding community, as described elsewhere [27]. Exclusion criteria included a reported history of chronic diseases or medications known to affect nutrition or bone health, including HIV infection and chronic liver disease.

### Assessment of Demographic, Clinical, and Anthropometric Data

Demographic and clinical data were collected from coinfecting, HCV-monoinfected, and HIV-monoinfected participants using a structured questionnaire. Data included age; race and ethnicity; current smoking status; alcohol use, determined with the Alcohol Use Disorders Identification Test questionnaire [28, 29]; diabetes; postmenopausal status (absence of menstrual periods for  $>12$  months in a woman aged  $>45$  years); and calcium and vitamin D supplement use. Physical activity was measured with the Multi-Ethnic Study of Atherosclerosis (MESA) physical activity questionnaire [30]. Minutes of activity in a typical week were summed for each activity type, converted to hours, and multiplied by metabolic equivalent (MET) level [30, 31]. Total MET-hours per week of activity and intentional exercise were determined.

For HIV-infected participants, records were reviewed to determine HIV transmission risk factors and most recent CD4 cell count, HIV RNA, hepatitis B surface antigen (HBsAg), serum

creatinine, and ART regimen. For chronically HCV-infected participants, we collected the most recent HBsAg, HCV RNA, creatinine, and METAVIR stage of hepatic fibrosis by liver biopsy [32], HCV FibroSure test (Laboratory Corporation of America, Burlington, North Carolina) [33], or Hepascore test (Quest Diagnostics, San Juan Capistrano, California) [34]. For the healthy female reference group, data were available on age, race, ethnicity, current smoking, physical activity (based on MESA questionnaire), and postmenopausal status. Body weight and height were measured using a digital scale (Scaltronix) and stadiometer (Holtain), respectively. Body mass index (BMI) was calculated as weight in kilograms divided by height in meters squared.

### pQCT Measurements

Bone measurements in the left tibia were obtained by means of pQCT (Stratec XCT2000 12-detector unit; Orthometrix) with a voxel size of 0.4 mm, and were analyzed with Stratec software (version 6.00). A scout view was obtained to place the reference line at the medial distal end-plate border. Bone measurements were obtained at 3% and 38% of tibia length proximal to the reference line. At the 3% metaphyseal site, scans were analyzed for trabecular volumetric BMD (in milligrams per cubic centimeter). At the 38% diaphyseal site, scans were analyzed for cortical volumetric BMD (milligrams per cubic centimeter), cortical cross-sectional area (square millimeters), and cortical thickness, periosteal circumference, and endosteal circumference (all in millimeters). Quality control was monitored daily using a hydroxyapatite phantom. The coefficient of variation (CV) was 0.5%–1.6%.

### Whole-Body DXA Measurements

Areal BMD at the total hip and femoral neck and whole-body fat and lean mass were assessed by means of DXA using a Hologic densitometer (Delphi/Discovery Systems; Hologic). Participants with BMD below the expected range for age and sex were identified by *z* scores of  $-2.0$  or less [35]. Measurements were performed in the array mode using standard positioning techniques. Quality control was monitored daily using a phantom. The CV was  $<1\%$  [36]. Appendicular lean mass, a measure of skeletal muscle [37], and whole-body fat mass were converted to appendicular lean mass index and fat mass index (both in kilograms per square meter) using height.

### Laboratory Data

Blood samples were collected for determination of serum calcium and phosphate, measured using standard clinical methods with CVs of 1.3% and 2.1%, respectively [38]. Intact parathyroid hormone (PTH) was measured using an automated immunochemical assay with a CV of 3%–6%. Serum 25(OH)D and 1,25-dihydroxyvitamin D ( $1,25[\text{OH}]_2\text{D}$ ) were measured using immunoaffinity enrichment and liquid chromatography-tandem mass spectrometry with interassay CVs of 3%–5% and 10%–11%,

respectively [39–41]. Intact fibroblast growth factor 23 (FGF23), which regulates  $1,25(\text{OH})_2\text{D}$  and phosphate levels [42], was measured using enzyme-linked immunosorbent assay (Kainos Laboratories; CV, 6%–11%). TNF- $\alpha$ , IL-1 $\beta$ , and IL-6 were measured using a high-sensitivity multiplex assay on an electrochemiluminescence platform (Meso Scale Discovery), with intra-assay CVs of 10.5%, 7.2%, and 5.9%, respectively.

### Statistical Analysis

We first converted pQCT and DXA measurements to sex- and race-specific (black vs nonblack) *z* scores relative to age to facilitate comparisons across the age range and between racial groups. The *z* scores were generated using the LMS method [43] based on curves generated with the data from the 263 reference participants. The LMS method accounts for the nonlinearity, heteroscedasticity, and skew of bone and body composition data with age [37]. Cortical dimension *z* scores were further adjusted for tibia length [44]. The age and race distributions of the reference participants were selected for the purpose of generating reference curves, and differed in comparisons with the 3 infected groups. Sex, race, and age-specific *z* scores were generated for all bone and body composition outcomes.

We determined differences in body composition between coinfecting, HCV-monoinfected, HIV-monoinfected, and reference participants using whole-body DXA. We used multivariable linear regression to determine whether appendicular lean mass index and whole-body fat mass index *z* scores were associated with pQCT and DXA bone measurements within each group.

Next, we determined differences in mean pQCT and DXA bone *z* scores in (1) coinfecting versus reference participants, (2) coinfecting versus HCV-monoinfected, (3) coinfecting versus HIV-monoinfected, and (4) HCV- and HIV-monoinfected versus reference participants. We evaluated postmenopausal status as an effect modifier, given its impact on bone health. We also determined whether coinfecting patients with a history of injection drug use more commonly had bone abnormalities than those without this history. Because Baker et al [27] had reported that lean mass was positively associated with trabecular volumetric BMD and cortical area and negatively associated with cortical volumetric BMD in the reference group, we performed multivariable linear regression, adjusting for appendicular lean mass index and whole-body fat mass index *z* scores. Analyses were also adjusted for smoking and physical activity, because we observed significant differences in these variables across the groups.

Among chronically HCV-infected patients, we used multivariable linear regression to determine whether advanced hepatic fibrosis/cirrhosis (METAVIR stage 3–4 fibrosis) and high HCV RNA levels ( $\geq 800\,000$  IU/mL) were associated with larger mean differences in pQCT and DXA bone *z* scores, after adjustment for appendicular lean mass index and fat mass index *z* scores, smoking, and physical activity.

Analyses were performed using Stata 13.0 software (Stata Corp). Although multiple comparisons were performed across numerous correlated bone measurements, Bonferroni correction was not appropriate because it assumes that these measurements are independent. We interpreted findings with caution and examined the consistency of results.

## RESULTS

### Participant Characteristics

50 HIV/HCV-coinfected, 51 HCV-monoinfected, and 50 HIV-monoinfected participants were enrolled. Their characteristics, along with those of the 263 reference participants, are summarized in Table 1. HIV-monoinfected patients were younger and less commonly reported current smoking than coinfecting or HCV-monoinfected participants. No differences were observed across the 3 infected groups in alcohol use, postmenopausal status, diabetes, HBsAg, or calcium/vitamin D use. Median HCV RNA levels and prevalence of advanced hepatic fibrosis/cirrhosis were similar between coinfecting and HCV-monoinfected participants. Coinfecting patients were less commonly black and more frequently reported injection drug use and blood transfusion as HIV risk factors than HIV-monoinfected participants. No differences in HIV suppression, median CD4 cell count, or use of antiretrovirals, including tenofovir, were observed between coinfecting and HIV-monoinfected participants. The reference group was more commonly white and had higher median total physical activity (in MET-hours per week) than the 3 infected groups.

### Group Differences in Body Composition

#### *HIV/HCV-Coinfected Versus Reference Participants*

In comparisons stratified on race, coinfecting and reference participants had comparable BMI (Table 1). Race-specific appendicular lean mass index and whole-body fat mass index  $z$  scores also did not differ (Table 2).

#### *HIV/HCV-Coinfected Versus HCV- and HIV-Monoinfected Participants*

Coinfecting participants had lower mean appendicular lean mass index and whole-body fat mass index  $z$  scores than HCV- and HIV-monoinfected participants (Table 2). In analyses stratified on race, coinfecting patients had a lower median BMI, but group differences were not statistically significant.

#### *HCV- and HIV-monoinfected Versus Reference Participants*

Mean appendicular lean mass index and fat mass index  $z$  scores were higher in HCV- and HIV-monoinfected than in reference participants (Table 2). In analyses stratified on race, HCV- and HIV-monoinfected patients had higher median BMIs than reference participants ( $P < .05$ ).

### Associations Between Body Composition and Bone Measurements

Within each of the 4 groups, appendicular lean mass index  $z$  scores were positively associated with all pQCT and DXA bone measurements ( $P < .01$ ), independent of fat mass index  $z$  scores. No associations were observed between fat mass index  $z$  scores and pQCT and DXA bone measurements, after controlling for appendicular lean mass index  $z$  scores.

### Group Differences in Bone Measurements

#### *HIV/HCV-Coinfected Versus Reference Participants*

With pQCT, mean trabecular volumetric BMD, cortical volumetric BMD, cortical area, and cortical thickness  $z$  scores were lower in coinfecting than in reference participants (Table 2). The smaller cortical dimensions were due to significantly greater  $z$  scores for endosteal circumference, with comparable  $z$  scores for periosteal circumference. Adjustment for appendicular lean mass index and fat mass index  $z$  scores, smoking, and total physical activity did not change results (Supplementary Table 1). Postmenopausal status increased differences between coinfecting and reference participants in  $z$  scores for cortical volumetric BMD ( $-1.01$  vs  $-0.16$ ) and cortical area ( $-0.89$  vs  $0.02$ ;  $P < .05$  for both interactions).

Mean total hip and femoral neck BMD  $z$  scores at DXA were lower in coinfecting participants (Table 2). Higher proportions of coinfecting women had low BMD for age ( $z$  score,  $-2.0$  or less) at the total hip (9 of 50 [18.0%] vs 6 of 263 [2.3%];  $P < .001$ ) and femoral neck (5 of 50 [10.0%] vs 5 of 263 [1.9%];  $P < .001$ ). There were no differences in pQCT or DXA bone measurements between those who reported a history of injection drug use and those who did not (data not shown).

#### *HIV/HCV-Coinfected Versus HCV- and HIV-Monoinfected Participants*

Mean trabecular volumetric BMD (Figure 1) and cortical thickness  $z$  scores at pQCT were lower in coinfecting than in HCV- and HIV-monoinfected participants (Table 2). After adjustment for the appendicular lean mass index and fat mass index  $z$  scores, smoking, and physical activity, differences in trabecular volumetric BMD were attenuated and differences in cortical thickness were no longer significant in the comparison with HCV-monoinfected (Supplementary Table 2) and HIV-monoinfected (Supplementary Table 3) participants.

Mean total hip and femoral neck BMD  $z$  scores at DXA were similar between coinfecting and HCV-monoinfected patients (Table 2). Similar proportions of coinfecting and HCV-monoinfected patients had low BMD for age at the total hip (9 of 50 [18.0%] vs 6 of 51 [11.7%];  $P = .40$ ) and femoral neck (5 of 50 [10.0%] vs 4 of 51 [7.8%];  $P = .75$ ).

Coinfecting participants had lower mean total hip and femoral neck BMD  $z$  scores than HIV-monoinfected participants (Table 2). There were no significant differences between

**Table 1. Characteristics of HIV/Chronically HCV-Coinfected, Chronically HCV-Monoinfected, HIV-Monoinfected, and Healthy Female Reference Participants**

Characteristic	HIV/HCV-Coinfected (n = 50)	HCV-Monoinfected (n = 51)	HIV-Monoinfected (n = 50)	Healthy Reference (n = 263)	P Value		
					HIV/HCV vs HCV	HIV/HCV vs HIV	HIV/HCV vs Reference
Age, median (IQR), y	51 (46–56)	55 (50–60)	47 (40–52)	47 (36–60)	.01	.004	.1
Race, No. (%)					.2 <sup>a</sup>	.02 <sup>a</sup>	<.001 <sup>a</sup>
Black	39 (78)	43 (84)	42 (84)	112 (42)			
White	11 (22)	6 (12)	4 (8)	136 (52)			
Other	0 (0)	2 (4)	4 (8)	15 (6)			
Hispanic, No. (%)	1 (2)	1 (2)	4 (8)	4 (2)	>.99 <sup>a</sup>	.4 <sup>a</sup>	.6 <sup>a</sup>
BMI, median (IQR), kg/m <sup>2</sup>							
Black	29.2 (25.5–33.0)	31.3 (27.7–35.3)	31.9 (26.4–36.8)	28.6 (24.8–33.6)	.1	.2	.5
White	24.1 (22.2–27.7)	29.8 (26.7–34.9)	31.0 (24.3–36.7)	23.3 (20.6–27.2)	.08	.2	.9
Current smoker, No. (%)	40 (80)	25 (49)	16 (32)	35 (13)	.001	<.001	<.001
Physical activity, mean (SD), MET-h/wk							
Total	171.0 (127.6)	180.9 (104.4)	203.7 (108.3)	268.7 (197.5)	.7	.2	<.001
Intentional exercise	21.5 (28.3)	21.7 (24.2)	24.1 (37.7)	46.6 (72.7)	.9	.7	<.001
Alcohol use, median (IQR), AUDIT score	0 (0–2)	0 (0–3)	1 (0–2)	...	.6	.2	...
Postmenopausal, No. (%) <sup>b</sup>	33 (66)	38 (75)	24 (48)	125 (48)	.3	.1	.01
Type 2 diabetes mellitus, No. (%)	9 (18)	17 (33)	4 (8)	...	.08	.2 <sup>a</sup>	...
Receiving calcium, No. (%)	10 (20)	16 (31)	11 (22)	...	.2	.8	...
Receiving vitamin D, No. (%)	12 (24)	18 (35)	12 (24)	...	.2	>.99	...
Serum creatinine, median (IQR), mg/dL	0.82 (0.70–0.92)	0.77 (0.68–0.96)	0.82 (0.75–0.95)	...	.7	.4	...
HBsAg positive, No. (%)	3 (6)	5 (10)	1 (2)	...	.6	.3	...
HCV RNA, median (IQR), log IU/mL	6.3 (5.9–6.8)	6.4 (5.8–6.8)	...	...	.8	...	...
METAVIR fibrosis stage, No. (%)					.8	...	...
0–2	38 (76)	40 (78)	...	...			
3–4	12 (24)	11 (22)	...	...			
METAVIR inflammation grade, No. (%)					.7	...	...
0–1	32 (64)	30 (59)	...	...			
2–3	18 (36)	21 (41)	...	...			
HIV RNA <75 copies/mL, No. (%)	43 (86)	...	37 (74)	...	...	.1	...
CD4 cell count, median (IQR), cells/mm <sup>3</sup>	605 (451–805)	...	635 (458–830)	...	...	.8	...
HIV risk factor, No. (%)							
Injection drug use	17 (34)	...	0 (0)	...	...	<.001	...
Unprotected sex	34 (68)	...	47 (94)	...	...	.002	...
Transfusion	3 (6)	...	0 (0)	...	...	.08	...
Other	2 (4)	...	3 (6)	...	...	.5 <sup>a</sup>	...
ART use, No. (%)							
NRTI	44 (88)	...	50 (100)	...	...	.03 <sup>a</sup>	...
NNRTI	16 (32)	...	20 (40)	...	...	.4	...
Protease inhibitor	18 (36)	...	27 (54)	...	...	.07	...
Integrase inhibitor	10 (20)	...	6 (12)	...	...	.3	...
Tenofovir	35 (70)	...	39 (78)	...	...	.4	...

Abbreviations: ART, antiretroviral therapy; AUDIT, Alcohol Use Disorders Identification Test-Consumption; BMI, body mass index; HBsAg, hepatitis B surface antigen; HCV, hepatitis C virus; HIV, human immunodeficiency virus; IQR, interquartile range; MET-h, metabolic-equivalent hours; NNRTI, nonnucleoside reverse transcriptase inhibitor; NRTI, nucleoside reverse-transcriptase inhibitor; SD, standard deviation.

<sup>a</sup> P value determined by Fisher exact test.

<sup>b</sup> Postmenopausal status was defined as the absence of menstrual periods for >12 months in a woman aged >45 years.



**Table 2. DXA and Tibial pQCT Measurements in HIV/HCV-Coinfected, HCV-Monoinfected, HIV-Monoinfected, and Healthy Female Reference Participants**

Bone Measurement	z Score, Mean (SD)				P Value		
	HIV/HCV Coinfected (n = 50)	HCV Monoinfected (n = 51)	HIV Monoinfected (n = 50)	Healthy Reference (n = 263)	HIV/HCV vs HCV	HIV/HCV vs HIV	HIV/HCV vs Reference
<b>pQCT</b>							
Trabecular vBMD	-0.85 (1.11)	-0.21 (1.03)	0.06 (1.36)	-0.01 (1.01)	.004	<.001	<.001
Cortical vBMD	-0.67 (1.10)	-0.36 (1.07) <sup>a</sup>	-0.40 (1.12) <sup>a</sup>	0.00 (1.00)	.16	.24	<.001
Cortical area	-0.61 (1.51)	-0.12 (1.07)	0.04 (0.99)	0.03 (0.93)	.07	.01	<.001
Cortical thickness	-0.77 (1.39)	-0.26 (1.07)	-0.22 (1.04)	0.00 (0.99)	.04	.03	<.001
Periosteal circumference	0.04 (1.07)	-0.03 (1.20)	0.31 (0.78) <sup>a</sup>	0.01 (0.89)	.77	.15	.87
Endosteal circumference	0.67 (1.37)	0.25 (0.95)	0.45 (0.94) <sup>a</sup>	0.07 (0.96)	.08	.37	<.001
<b>DXA</b>							
Total hip BMD	-0.89 (1.27)	-0.62 (1.12) <sup>a</sup>	-0.18 (1.18)	0.00 (1.00)	.27	.005	<.001
Femoral neck BMD	-0.81 (1.10)	-0.56 (1.17) <sup>a</sup>	-0.23 (1.15)	0.00 (1.01)	.30	.01	<.001
Appendicular lean mass index	0.01 (1.11)	0.57 (1.01) <sup>a</sup>	0.55 (1.40) <sup>a</sup>	0.00 (1.01)	.01	.04	.91
Whole-body fat mass index	0.00 (1.26)	0.56 (1.03) <sup>a</sup>	0.52 (1.36) <sup>a</sup>	0.00 (1.00)	.02	.05	.99

Abbreviations: BMD, bone mineral density; DXA, dual-energy x-ray absorptiometry; HCV, hepatitis C virus; HIV, human immunodeficiency virus; pQCT, peripheral quantitative computed tomography; SD, standard deviation; vBMD, volumetric BMD.

<sup>a</sup> P < .05 for comparison with healthy female reference participants.

coinfected and HIV-monoinfected participants in the prevalence of low BMD for age at the total hip (9 of 50 [18.0%] vs

4 of 50 [8.0%]; P = .14) or femoral neck (5 of 50 [10.0%] vs 4 of 50 [8.0%]; P = .73).

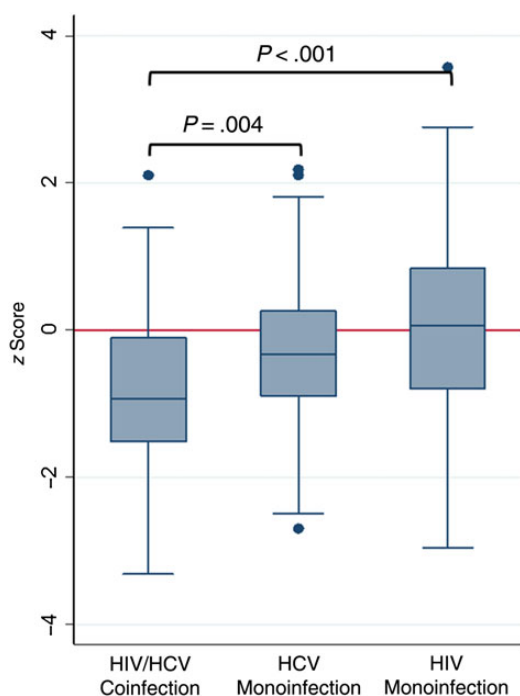


**Figure 1.** Mean trabecular volumetric bone mineral density z scores for antiretroviral-treated human immunodeficiency virus (HIV)/hepatitis C virus (HCV)-coinfected, HCV-monoinfected, and antiretroviral-treated HIV-monoinfected female participants.

#### HCV- and HIV-Monoinfected vs Healthy Reference Participants

HCV-monoinfected participants had lower mean cortical volumetric BMD, total hip BMD, and femoral neck BMD z scores than the reference group. After adjustment for appendicular lean mass index and fat mass index z scores, smoking, and physical activity, trabecular volumetric BMD, cortical area, cortical thickness, periosteal circumference, total hip BMD, and femoral neck BMD z scores remained lower in HCV-monoinfected patients (Supplementary Table 4). Postmenopausal status did not increase differences in pQCT measurements between HCV-monoinfected and reference participants.

HIV-monoinfected patients had lower cortical volumetric BMD and higher mean periosteal and endosteal circumference z scores than reference participants. After adjustment for appendicular lean mass index and fat mass index z scores, smoking, and physical activity, HIV-monoinfected patients had lower cortical thickness, higher endosteal circumference, and lower total hip and femoral neck z scores (Supplementary Table 5). Postmenopausal status increased differences between HIV-monoinfected and reference participants only in cortical thickness z scores (-0.61 vs -0.03; P < .05 for interaction).

#### Inflammatory Cytokines and Vitamin D-Related Metabolism

TNF- $\alpha$  levels were significantly higher in coinfecting than in HCV- or HIV-monoinfected participants. There were no differences

**Table 3. Mineral Metabolism and Inflammatory Cytokine Levels in HIV/HCV-Coinfected, HCV-Monoinfected, and HIV-Monoinfected Women**

Laboratory Measurement	Median Value (IQR)			P Value	
	HIV/HCV Coinfected (n = 50)	HCV Monoinfected (n = 51)	HIV Monoinfected (n = 50)	HIV/HCV vs HCV	HIV/HCV vs HIV
<b>Vitamin D metabolism</b>					
Serum calcium, mg/dL	10.0 (9.5–10.4)	10.3 (9.8–10.8)	10.1 (9.5–10.6)	.22	.25
Serum phosphate, mg/dL	3.6 (3.3–3.9)	3.7 (3.3–4.1)	3.7 (3.1–4.3)	.29	.85
PTH, pg/mL	36.1 (28.3–47.2)	38.6 (27.2–50.2)	40.9 (31.5–64.8)	.45	.03
25(OH)D, ng/mL	23.5 (13.6–35.8)	24.7 (16.8–36.5)	25.4 (13.4–35.9)	.45	.95
1,25(OH) <sub>2</sub> D, ng/mL	51.7 (33.7–72.6)	46.3 (37.3–67.4)	52.8 (39.4–71.3)	.81	.53
FGF23, pg/mL	35.4 (25.0–43.9)	41.3 (25.0–54.3)	28.9 (20.5–37.7)	.22	.13
<b>Inflammatory cytokines</b>					
IL-1 $\beta$ , pg/mL	0.12 (0.12–0.31)	0.12 (0.12–0.18)	0.12 (0.12–0.18)	.34	.25
IL-6, pg/mL	1.45 (1.15–2.06)	1.65 (0.92–2.25)	1.06 (0.76–1.67)	.99	.06
TNF- $\alpha$ , pg/mL	3.11 (2.53–3.85)	2.64 (2.10–3.46)	2.05 (1.66–2.73)	.04	<.001

Abbreviations: 1,25(OH)<sub>2</sub>D, 1,25-hydroxyvitamin D; 25(OH)D, 25-hydroxyvitamin D; FGF23, fibroblast growth factor 23; HCV, hepatitis C virus; HIV, human immunodeficiency virus; IL-1 $\beta$ , interleukin 1 $\beta$ ; IL-6, interleukin 6; IQR, interquartile range; PTH, parathyroid hormone; TNF, tumor necrosis factor.

in median serum calcium, phosphate, PTH, 25(OH)D, 1,25(OH)<sub>2</sub>D, FGF23, IL-1 $\beta$ , and IL-6 levels between coinfecting, HCV-monoinfected, and HIV-monoinfected participants (Table 3).

**Bone Measurements in HCV-Infected Patients, by Liver Fibrosis Stage and HCV RNA Level**

In multivariable linear regression analyses among chronically HCV-infected patients, those with stage 3–4 liver fibrosis had lower mean trabecular volumetric BMD, cortical thickness, and total hip BMD z scores than those with stage 0–2 fibrosis (Table 4). Serum 1,25(OH)<sub>2</sub>D levels were lower in patients with fibrosis stage 3–4 than in those with stage 0–2 (53.0 vs

40.7 ng/mL; *P* = .03), but there were no differences in calcium, phosphate, PTH, 25(OH)D, FGF23, IL-1 $\beta$ , IL-6, or TNF- $\alpha$  levels (data not shown). Mean cortical thickness z scores were lower and mean endosteal circumference z scores higher in participants with HCV RNA levels  $\geq$ 800 000 IU/mL (Table 4).

**DISCUSSION**

Our study found that ART-treated HIV/HCV-coinfecting women had substantially lower tibial trabecular volumetric BMD and diminished cortical dimensions with significant endocortical bone deficits, independent of appendicular lean mass

**Table 4. Differences (95% CIs) in Mean Tibia pQCT and DXA Bone z scores in Chronically HCV-Infected Female Participants by HCV RNA Level and METAVIR Fibrosis Stage**

Bone Measurement	Difference in Mean z Score (95% CI) for High vs Low HCV RNA <sup>a</sup>		Difference in Mean z Score (95% CI) for Fibrosis Stage 3–4 vs 0–2 <sup>a</sup>	
	95% CI	P Value	95% CI	P Value
<b>pQCT</b>				
Trabecular vBMD	−0.09 (−.54 to .35)	.67	−0.46 (−.88 to −.02)	.04
Cortical vBMD	−0.40 (−.88 to .08)	.11	−0.32 (−.82 to .18)	.20
Cortical area	−0.29 (−.78 to .20)	.25	−0.49 (−.99 to .02)	.06
Cortical thickness	−0.62 (−1.11 to −.13)	.01	−0.64 (−1.14 to −.14)	.01
Periosteal circumference	0.30 (−.19 to .79)	.22	−0.26 (−.77 to .24)	.31
Endosteal circumference	0.76 (.26 to 1.28)	.004	0.47 (−.07 to 1.01)	.10
<b>DXA</b>				
Total hip BMD	−0.12 (−.57 to .33)	.61	−0.46 (−.92 to −.01)	.04
Femoral neck BMD	−0.01 (−.45 to .44)	.99	−0.28 (−.73 to .18)	.23

Abbreviations: BMD, bone mineral density; CI, confidence interval; DXA, dual-energy x-ray absorptiometry; HCV, hepatitis C virus; pQCT, peripheral quantitative computed tomography; vBMD, volumetric BMD.

<sup>a</sup> Differences were adjusted for appendicular lean mass index and fat mass index z scores, current smoking, and physical activity. High HCV RNA levels were defined as  $\geq$ 800 000 IU/mL; low levels, as <800 000 IU/mL.

and fat mass, compared with healthy reference participants. The mean trabecular volumetric BMD  $z$  score of  $-0.85$  and mean cortical volumetric BMD and endosteal circumference  $z$  scores of  $-0.67$  (Table 1) indicate that the average female coinfecting participant had results at the 20th and 25th percentiles for these parameters, respectively, for age, sex, and race. Furthermore, tibial trabecular volumetric BMD was lower and median TNF- $\alpha$  levels higher in coinfecting women than in either HCV- or HIV-monoinfected women. Finally, chronically HCV-infected women with stage 3–4 liver fibrosis had lower mean trabecular volumetric BMD, cortical area, and cortical thickness  $z$  scores than HCV-infected women with stage 0–2 fibrosis.

The findings of decreased trabecular volumetric BMD and reduced tibial cortical dimensions with increased endosteal, but preserved periosteal, circumferences among coinfecting women, in the absence of hepatic decompensation, support the hypothesis that HIV- and HCV-mediated chronic inflammation might contribute to the structural bone deficits observed in this group. Studies of patients with other chronic inflammatory conditions, particularly inflammatory bowel disease [20, 21] and rheumatoid arthritis [22], have demonstrated a similar pattern of trabecular bone loss and endocortical thinning. The higher levels of TNF- $\alpha$  among coinfecting participants further suggests the contribution of chronic inflammation. This cytokine can reduce trabecular and cortical bone formation by inhibiting osteoblast differentiation, inhibiting osteoblast collagen secretion, and inducing osteoblast apoptosis [16, 17]. TNF- $\alpha$  can also promote accelerated trabecular and cortical bone resorption by inducing expression of receptor activator of nuclear factor kappa-B ligand (RANKL), which stimulates osteoclast activation and inhibits osteoblast apoptosis [45, 46].

Our results extend the observations of prior DXA studies in HIV/HCV patients [47, 48]. One study evaluated 179 HIV/HCV patients (35% female; 85% black) at Johns Hopkins University [47]. The prevalence of low BMD at the total hip, femoral neck, or lumbar spine among coinfecting females was 19.1%, similar to that observed in the present analysis. A subsequent study at Johns Hopkins evaluated bone strength, measured by DXA-derived hip structural analysis, in 88 coinfecting men compared with 289 age- and race-matched uninfected male controls [48]. Coinfecting men had compromised bone strength at the narrow neck and shaft of the proximal femur, and the smaller cortical area of the shaft coupled with normal bone width (ie, periosteal circumference) was consistent with endocortical bone deficits, similar to our findings with pQCT. Finally, 2 studies used high-resolution pQCT to evaluate bone microstructure in ART-treated HIV-infected premenopausal women [49] and young men [50], and both identified trabecular and cortical bone deficits compared with HIV-uninfected controls.

Appendicular lean mass was strongly associated with all pQCT measurements. Lean mass confers beneficial effects on BMD [51]. Lower lean mass was a determinant of regional

bone mineral content via DXA in ART-treated HIV-infected men [52] and was associated with reduced total hip BMD in HIV/HCV-coinfecting men [48]. Reductions in lean mass may be partially reversible with ART [53], but may persist after HIV suppression, possibly owing to HIV-related inflammation [54].

We observed that HCV-infected women with advanced hepatic fibrosis/cirrhosis had lower mean trabecular volumetric BMD, cortical area, and cortical thickness than those with stage 0–2 liver fibrosis. These results suggest that advanced hepatic fibrosis, in the absence of hepatic decompensation, negatively affects bone mass and quality. This finding might reflect the prolonged impact of chronic HCV-associated systemic inflammation on bone.

Our study had several limitations. First, the cross-sectional design did not allow us to evaluate changes in pQCT measurements and other osteoporosis risk factors over time. Second, our analyses did not account for durations of HIV and chronic HCV, duration of ART use, history of injection drug/alcohol abuse, or poor nutrition, and these factors might be important contributors to bone deficits. Third, we did not have laboratory data to confirm the absence of HIV infection or viral hepatitis among reference participants. Finally, our results are generalizable only to women, but bone deficits with HIV/HCV coinfection have also been described in men [47, 48]. Future studies should examine pQCT measurements in coinfecting men.

In conclusion, ART-treated HIV/HCV-coinfecting women had decreased tibial trabecular volumetric BMD, significant endocortical bone loss, and increased TNF- $\alpha$  levels. Future studies should evaluate HIV/HCV-coinfecting men, examine changes in bone structure over time, and determine whether virologic cure after HCV therapy can improve BMD and reverse bone deficits.

## Supplementary Data

Supplementary materials are available at *The Journal of Infectious Diseases* online (<http://jid.oxfordjournals.org>). Supplementary materials consist of data provided by the author that are published to benefit the reader. The posted materials are not copyedited. The contents of all supplementary data are the sole responsibility of the authors. Questions or messages regarding errors should be addressed to the author.

## Notes

**Acknowledgments.** We appreciate the efforts of Ranjeeta Bahirwani, MD, Kimberly A. Forde, MD, MHS, David Goldberg, MD, MSCE, Karen Krok, MD, George Makar, MD, and K. Rajender Reddy, MD for their assistance in the recruitment of hepatitis C virus-monoinfected participants. We also thank the Penn Center for AIDS Research for their support during this study and all study participants for their participation.

**Financial support.** This work was supported by the Penn Center for AIDS Research (developmental pilot grant to V. L. R.), the National Institutes of Health (grant P30 AI 045008 and research grant K01-AI070001 to V. L. R.); the National Center for Research Resources (grant UL1 RR024134 to M. B. L.), and the National Center for Advancing Translational Sciences (grant UL1 TR000003 to M. B. L.).



**Potential conflicts of interest.** V. L. R. has received investigator-initiated research grant support (to the University of Pennsylvania) from AstraZeneca and Gilead Sciences. A. J. K. has served as a consultant to AbbVie and Gilead Sciences and served on the speakers bureau of AbbVie. K. M. has served as a consultant to Gilead Sciences, Johnson & Johnson, and Viiv; received research grant support from Gilead Sciences and Johnson & Johnson; and served on the speakers bureau of Bristol-Myers Squibb, Gilead Sciences, Johnson & Johnson, and Merck. J. R. K. has served as a consultant to AbbVie and Gilead Sciences. All other authors report no potential conflicts.

All authors have submitted the ICMJE Form for Disclosure of Potential Conflicts of Interest. Conflicts that the editors consider relevant to the content of the manuscript have been disclosed.

## References

- Brown TT, Qaqish RB. Antiretroviral therapy and the prevalence of osteopenia and osteoporosis: a meta-analytic review. *AIDS* **2006**; 20:2165–74.
- Brown TT, Chen Y, Currier JS, et al. Body composition, soluble markers of inflammation, and bone mineral density in antiretroviral therapy-naïve HIV-1-infected individuals. *J Acquir Immune Defic Syndr* **2013**; 63:323–30.
- Rouillard S, Lane NE. Hepatic osteodystrophy. *Hepatology* **2001**; 33:301–7.
- Leslie WD, Bernstein CN, Leboff MS. AGA technical review on osteoporosis in hepatic disorders. *Gastroenterology* **2003**; 125:941–66.
- van Vonderen MG, Lips P, van Agtmael MA, et al. First line zidovudine/lamivudine/lopinavir/ritonavir leads to greater bone loss compared to nevirapine/lopinavir/ritonavir. *AIDS* **2009**; 23:1367–76.
- Stellbrink HJ, Orkin C, Arribas JR, et al. Comparison of changes in bone density and turnover with abacavir-lamivudine versus tenofovir-emtricitabine in HIV-infected adults: 48-week results from the ASSERT study. *Clin Infect Dis* **2010**; 51:963–72.
- McComsey GA, Kitch D, Daar ES, et al. Bone mineral density and fractures in antiretroviral-naïve persons randomized to receive abacavir-lamivudine or tenofovir disoproxil fumarate-emtricitabine along with efavirenz or atazanavir-ritonavir. *AIDS Clinical Trials Group A5224a, a substudy of ACTG A5202. J Infect Dis* **2011**; 203:1791–801.
- Womack JA, Goulet JL, Gibert C, et al. Increased risk of fragility fractures among HIV infected compared to uninfected male veterans. *PLoS One* **2011**; 6:e17217.
- Young B, Dao CN, Buchacz K, Baker R, Brooks JT. Increased rates of bone fracture among HIV-infected persons in the HIV Outpatient Study (HOPS) compared with the US general population, 2000–2006. *Clin Infect Dis* **2011**; 52:1061–8.
- Lo Re V 3rd, Volk J, Newcomb CW, et al. Risk of hip fracture associated with hepatitis C virus infection and hepatitis C/human immunodeficiency virus coinfection. *Hepatology* **2012**; 56:1688–98.
- Anastos K, Lu D, Shi O, et al. The association of bone mineral density with HIV infection and antiretroviral treatment in women. *Antivir Ther* **2007**; 12:1049–58.
- Lo Re V 3rd, Guaraldi G, Leonard MB, et al. Viral hepatitis is associated with reduced bone mineral density in HIV-infected women but not men. *AIDS* **2009**; 23:2191–8.
- Yin MT, McMahon DJ, Ferris DC, et al. Low bone mass and high bone turnover in postmenopausal human immunodeficiency virus-infected women. *J Clin Endocrinol Metab* **2010**; 95:620–9.
- Lawson-Ayayi S, Cazanave C, Kpozehouen A, et al. Chronic viral hepatitis is associated with low bone mineral density in HIV-infected patients, ANRS CO 3 Aquitaine Cohort. *J Acquir Immune Defic Syndr* **2013**; 62:430–5.
- McComsey GA, Tebas P, Shane E, et al. Bone disease in HIV infection: a practical review and recommendations for HIV care providers. *Clin Infect Dis* **2010**; 51:937–46.
- Gilbert L, He X, Farmer P, et al. Expression of the osteoblast differentiation factor RUNX2 (Cbfa1/AML3/Pebp2alpha A) is inhibited by tumor necrosis factor-alpha. *J Biol Chem* **2002**; 277:2695–701.
- Radeff JM, Nagy Z, Stern PH. Involvement of PKC-beta in PTH, TNF-alpha, and IL-1 beta effects on IL-6 promoter in osteoblastic cells and on PTH-stimulated bone resorption. *Exp Cell Res* **2001**; 268:179–88.
- Kontulainen SA, Johnston JD, Liu D, Leung C, Oxland TR, McKay HA. Strength indices from pQCT imaging predict up to 85% of variance in bone failure properties at tibial epiphysis and diaphysis. *J Musculoskelet Neuronal Interact* **2008**; 8:401–9.
- Liu D, Manske SL, Kontulainen SA, et al. Tibial geometry is associated with failure load ex vivo: a MRI, pQCT and DXA study. *Osteoporos Int* **2007**; 18:991–7.
- Dubner SE, Shults J, Baldassano RN, et al. Longitudinal assessment of bone density and structure in an incident cohort of children with Crohn's disease. *Gastroenterology* **2009**; 136:123–30.
- Tsampalieros A, Lam CK, Spencer JC, et al. Long-term inflammation and glucocorticoid therapy impair skeletal modeling during growth in childhood Crohn disease. *J Clin Endocrinol Metab* **2013**; 98:3438–45.
- Aeberli D, Eser P, Bonel H, et al. Reduced trabecular bone mineral density and cortical thickness accompanied by increased outer bone circumference in metacarpal bone of rheumatoid arthritis patients: a cross-sectional study. *Arthritis Res Ther* **2010**; 12:R119.
- Alter MJ, Kruszon-Moran D, Nainan OV, et al. The prevalence of hepatitis C virus infection in the United States, 1988 through 1994. *N Engl J Med* **1999**; 341:556–62.
- Sherman KE, Rouster SD, Chung RT, Rajicic N. Hepatitis C virus prevalence among patients infected with human immunodeficiency virus: a cross-sectional analysis of the US adult AIDS Clinical Trials Group. *Clin Infect Dis* **2002**; 34:831–7.
- Amorosa V, Tebas P. Bone disease and HIV infection. *Clin Infect Dis* **2006**; 42:108–14.
- Hofmann WP, Kronenberger B, Bojunga J, et al. Prospective study of bone mineral density and metabolism in patients with chronic hepatitis C during pegylated interferon alpha and ribavirin therapy. *J Viral Hepat* **2008**; 15:790–6.
- Baker JF, Davis M, Alexander R, et al. Associations between body composition and bone density and structure in men and women across the adult age spectrum. *Bone* **2013**; 53:34–41.
- Isaacson JH, Butler R, Zacharek M, Tzelepis A. Screening with the Alcohol Use Disorders Identification Test (AUDIT) in an inner-city population. *J Gen Intern Med* **1994**; 9:550–3.
- Bush K, Kivlahan DR, McDonell MB, Fihn SD, Bradley KA. The AUDIT alcohol consumption questions (AUDIT-C): an effective brief screening test for problem drinking. Ambulatory Care Quality Improvement Project (ACQUIP). Alcohol Use Disorders Identification Test. *Arch Intern Med* **1998**; 158:1789–95.
- Bild DE, Bluemke DA, Burke GL, et al. Multi-ethnic study of atherosclerosis: objectives and design. *Am J Epidemiol* **2002**; 156:871–81.
- Ainsworth BE, Haskell WL, Whitt MC, et al. Compendium of physical activities: an update of activity codes and MET intensities. *Med Sci Sports Exerc* **2000**; 32(Suppl 9):S498–504.
- Bedossa P, Poynard T. An algorithm for the grading of activity in chronic hepatitis C: the METAVIR Cooperative Study Group. *Hepatology* **1996**; 24:289–93.
- Poynard T, Imbert-Bismut F, Munteanu M, et al. Overview of the diagnostic value of biochemical markers of liver fibrosis (FibroTest, HCV FibroSure) and necrosis (ActiTest) in patients with chronic hepatitis C. *Comp Hepatol* **2004**; 3:8.
- Adams LA, Bulsara M, Rossi E, et al. Hepascore: an accurate validated predictor of liver fibrosis in chronic hepatitis C infection. *Clin Chem* **2005**; 51:1867–73.
- The International Society for Clinical Densitometry. 2007 Official Positions and Pediatric Official Positions of the International Society for Clinical Densitometry. <http://www.iscd.org/wp-content/uploads/2012/10/ISCD2007OfficialPositions-Combined-AdultandPediatric.pdf>. Accessed 23 April 2014.

36. Leonard MB, Shults J, Elliott DM, Stallings VA, Zemel BS. Interpretation of whole body dual energy x-ray absorptiometry measures in children: comparison with peripheral quantitative computed tomography. *Bone* **2004**; 34:1044–52.
37. Kelly TL, Wilson KE, Heymsfield SB. Dual energy x-Ray absorptiometry body composition reference values from NHANES. *PLoS One* **2009**; 4:e7038.
38. Serum-calcium [editorial]. *Lancet* **1979**; 1:858–9.
39. Hoofnagle AN, Laha TJ, Donaldson TF. A rubber transfer gasket to improve the throughput of liquid-liquid extraction in 96-well plates: application to vitamin D testing. *J Chromatogr B Analyt* **2010**; 878:1639–42.
40. Strathmann FG, Laha TJ, Hoofnagle AN. Quantification of 1 $\alpha$ ,25-dihydroxy vitamin D by immunoextraction and liquid chromatography-tandem mass spectrometry. *Clin Chem* **2011**; 57:1279–85.
41. Laha TJ, Strathmann FG, Wang Z, de Boer IH, Thummel KE, Hoofnagle AN. Characterizing antibody cross-reactivity for immunoaffinity purification of analytes prior to multiplexed liquid chromatography-tandem mass spectrometry. *Clin Chem* **2012**; 58:1711–6.
42. Holick MF. Vitamin D deficiency. *N Engl J Med* **2007**; 357:266–81.
43. Cole TJ. The LMS method for constructing normalized growth standards. *Eur J Clin Nutr* **1990**; 44:45–60.
44. Tsampalieros A, Kalkwarf HJ, Wetzsteon RJ, et al. Changes in bone structure and the muscle-bone unit in children with chronic kidney disease. *Kidney Int* **2013**; 83:495–502.
45. Gilbert L, He X, Farmer P, et al. Inhibition of osteoblast differentiation by tumor necrosis factor- $\alpha$ . *Endocrinology* **2000**; 141:3956–64.
46. Lee SE, Chung WJ, Kwak HB, et al. Tumor necrosis factor- $\alpha$  supports the survival of osteoclasts through the activation of Akt and ERK. *J Biol Chem* **2001**; 276:49343–9.
47. El-Maouche D, Mehta SH, Sutcliffe C, et al. Controlled HIV viral replication, not liver disease severity associated with low bone mineral density in HIV/HCV co-infection. *J Hepatol* **2011**; 55:770–6.
48. Walker Harris V, Sutcliffe CG, Araujo AB, et al. Hip bone geometry in HIV/HCV-co-infected men and healthy controls. *Osteoporos Int* **2012**; 23:1779–87.
49. Calmy A, Chevalley T, Delhumeau C, et al. Long-term HIV infection and antiretroviral therapy are associated with bone microstructure alterations in premenopausal women. *Osteoporos Int* **2013**; 24:1843–52.
50. Yin MT, Lund E, Shah J, et al. Lower peak bone mass and abnormal trabecular and cortical microarchitecture in young men infected with HIV early in life. *AIDS* **2014**; 28:345–53.
51. Zhao LJ, Liu YJ, Liu PY, et al. Relationship of obesity with osteoporosis. *J Clin Endocrinol Metab* **2007**; 92:1640–6.
52. Rosenthal L, Falutz J. Bone mineral and soft-tissue changes in AIDS-associated lipodystrophy. *J Bone Miner Metab* **2005**; 23:53–7.
53. Dube MP, Parker RA, Mulligan K, et al. Effects of potent antiretroviral therapy on free testosterone levels and fat-free mass in men in a prospective, randomized trial: A5005s, a substudy of AIDS Clinical Trials Group Study 384. *Clin Infect Dis* **2007**; 45:120–6.
54. Shikuma CM, Zackin R, Sattler F, et al. Changes in weight and lean body mass during highly active antiretroviral therapy. *Clin Infect Dis* **2004**; 39:1223–30.